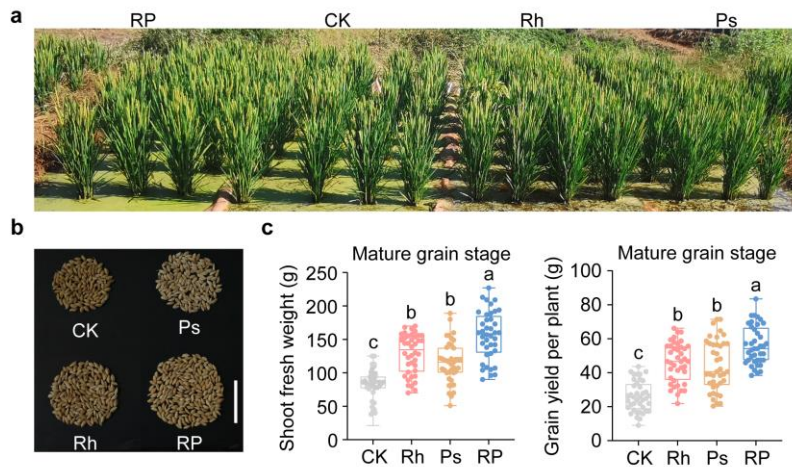
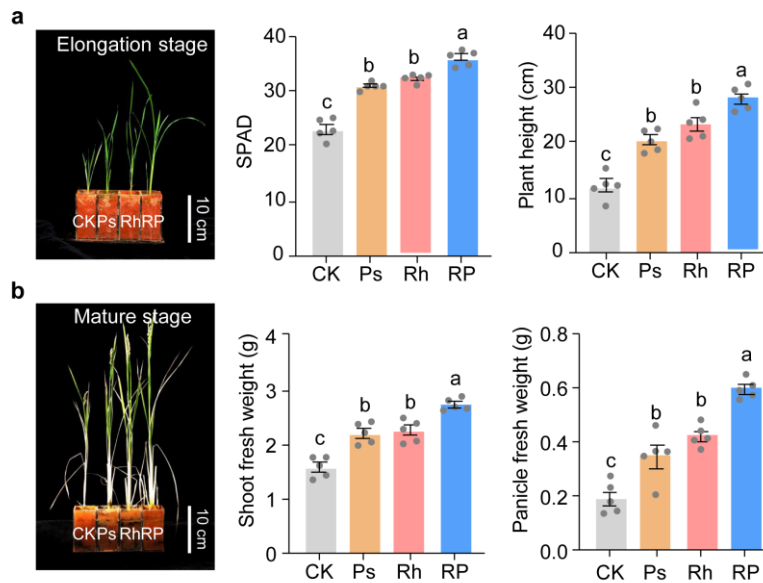


**Quinolone-mediated metabolic cross-feeding develops aluminium
tolerance in soil microbial consortia**

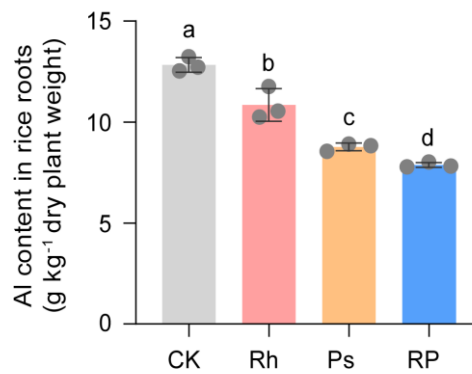
Ma et al.



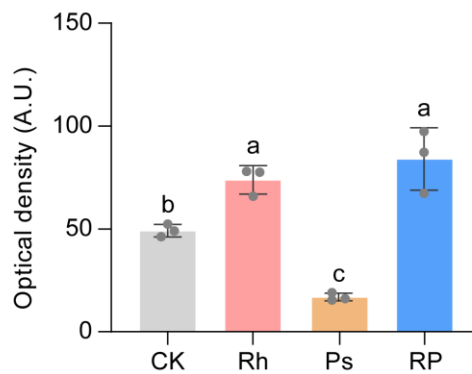
Supplementary Fig. 1. Promoting growth of rice Nanjing 46 under different treatments in the acidic field. **a**, Phenotypic observation results of aboveground parts at heading stage of rice. **b**, Phenotypic observation results of grain per panicle. **c**, Fresh shoot weight and yield per plant at maturity stage of rice (n = 40 biological replicates). In **c**, horizontal line inside the box plot represents the median, the top and bottom of the box represent the 75th and 25th percentiles, respectively, and the upper and lower error bars extend to the maximum and minimum values of the data range. Different letters indicate significant differences in variance analysis ($P < 0.05$, One-way ANOVA) after multiple comparisons (two-sided Fisher's LSD test). CK: non-inoculation, Rh: inoculation with *R. erythropolis*, Ps: inoculation with *P. aeruginosa*, RP: inoculation with co-cultured *R. erythropolis* and *P. aeruginosa*. Source data are provided as a Source Data file.



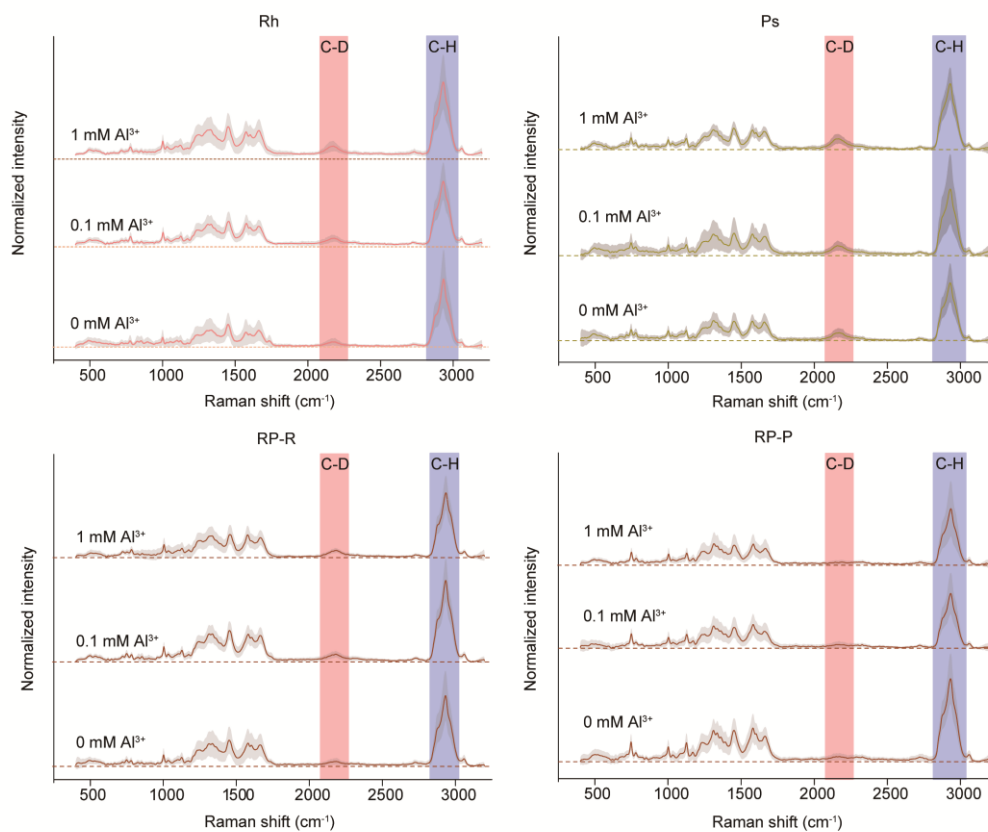
Supplementary Fig. 2. Promoting growth of potted rice Nanjing 46 under different treatments in acidic soil. **a**, Phenotypic observation results of aboveground parts, chlorophyll content, and plant height indicators at elongation stage of rice (n = 5 biological replicates, images representative of 5 experiments). **b**, Phenotypic observation results of aboveground parts, fresh shoot weight, and fresh panicle weight per plant at maturity stage of rice (n = 5 biological replicates, images representative of 5 experiments). Bar plots represent the average value, and error bars represent the standard deviation. Different letters indicate significant differences in variance analysis (one-way ANOVA, $P < 0.05$) after multiple comparisons (Two-sided Fisher's LSD test). CK: no-inoculation, Rh: inoculation with *R. erythropolis*, Ps: inoculation with *P. aeruginosa*, RP: inoculation with co-cultured *R. erythropolis* and *P. aeruginosa*. Source data are provided as a Source Data file.



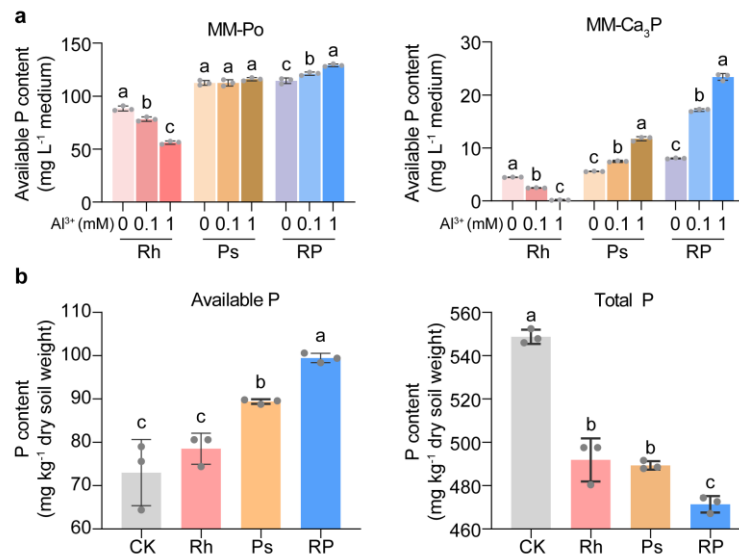
Supplementary Fig. 3. Al content in rice roots. Bar plots represent the average value, and error bars represent the standard deviation (n = 3 biological replicates). Different letters indicate significant differences in variance analysis (one-way ANOVA, $P < 0.05$) after multiple comparisons (Two-sided Fisher's LSD test). CK: no-inoculation, Rh: inoculation with *R. erythropolis*, Ps: inoculation with *P. aeruginosa*, RP: inoculation with co-cultured *R. erythropolis* and *P. aeruginosa*. Source data are provided as a Source Data file.



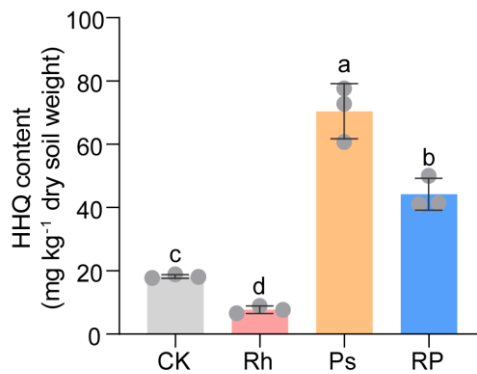
Supplementary Fig. 4. Fluorescence response of *R. erythropolis* in rhizosphere soil under different inoculation treatments. Optical density observation results of *R. erythropolis* fluorescence in rhizosphere soil (n = 3 biological replicates). Bar plots represent the average value, and error bars represent the standard deviation. Different letters indicate significant differences in variance analysis (one-way ANOVA, $P < 0.05$) after multiple comparisons (Two-sided Fisher's LSD test). CK: no-inoculation, Rh: inoculation with *R. erythropolis*, Ps: inoculation with *P. aeruginosa*, RP: inoculation with co-cultured *R. erythropolis* and *P. aeruginosa*, A. U.: arbitrary units. Source data are provided as a Source Data file.



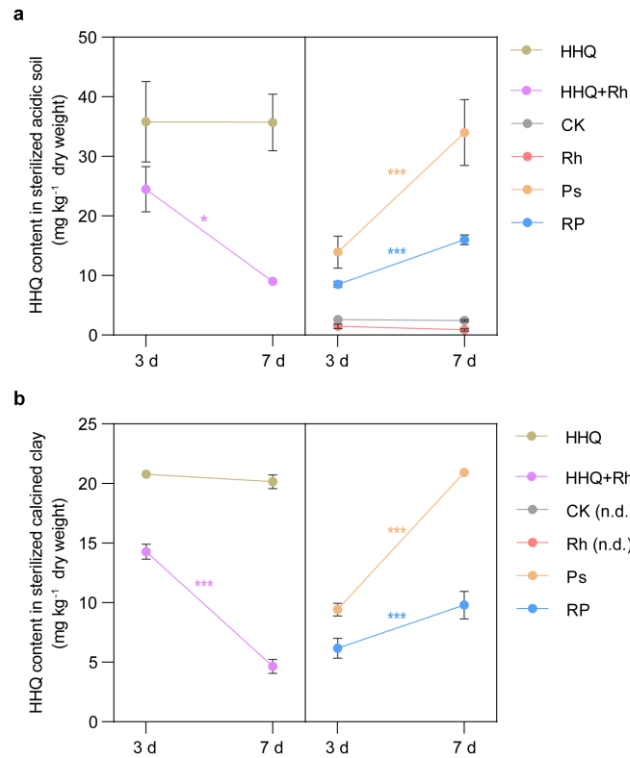
Supplementary Fig. 5. Metabolic activity of *R. erythropolis* and *P. aeruginosa* under mono-culture and co-culture at different Al^{3+} addition concentration by reverse-Raman- D_2O . The solid line in the center represents the average observed peak, and the shaded area represents the standard deviation ($n = 30$ biological replicates). C-D band represents the Raman peaks at 2,040-2,300 cm^{-1} , and C-H band represents the Raman peaks at 2,800-3,100 cm^{-1} . The Raman peak of cytochrome C at 749.95 cm^{-1} was selected as the fingerprint peak for identifying *P. aeruginosa* in co-culture. Rh: mono-culture of *R. erythropolis*, Ps: mono-culture of *P. aeruginosa*, RP-R: *R. erythropolis* in co-culture, RP-P: *P. aeruginosa* in co-culture. Source data are provided as a Source Data file.



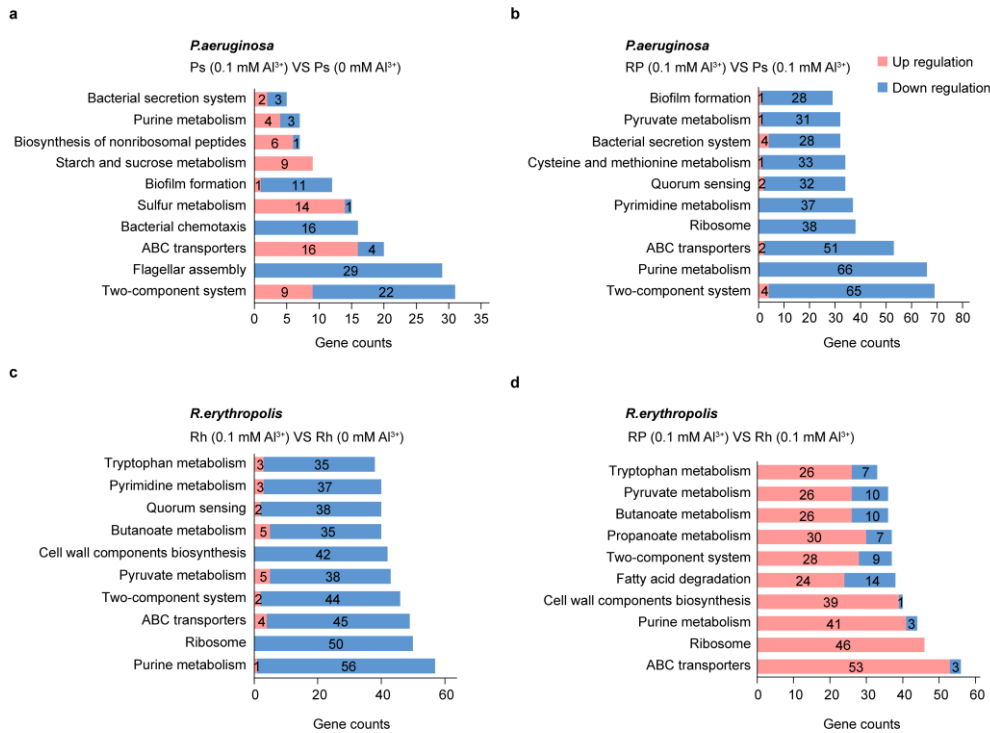
Supplementary Fig. 6. Phosphorus (P)-solubilizing efficacy of mono- and co-cultures. **a**, Quantification of available phosphate released from different P sources under Al gradients. **b**, Concentrations of soil available P and total P in pot experiments. Bar plots represent the average value, with error bars signifying the standard deviation ($n = 3$ biological replicates). Different letters denote significant differences in variance analysis (one-way ANOVA, $P < 0.05$) subsequent to multiple comparisons employing two-sided Fisher's LSD test. MM-Po: modified minimal media (MM) supplemented with sodium phytate as organic fixed P. MM-Ca₃P: MM supplemented with tricalcium phosphate as inorganic fixed P. CK: non-inoculation, Rh: inoculation with *R. erythropolis*, Ps: inoculation with *P. aeruginosa*, RP: inoculation with co-cultured *R. erythropolis* and *P. aeruginosa*. Source data are provided as a Source Data file.



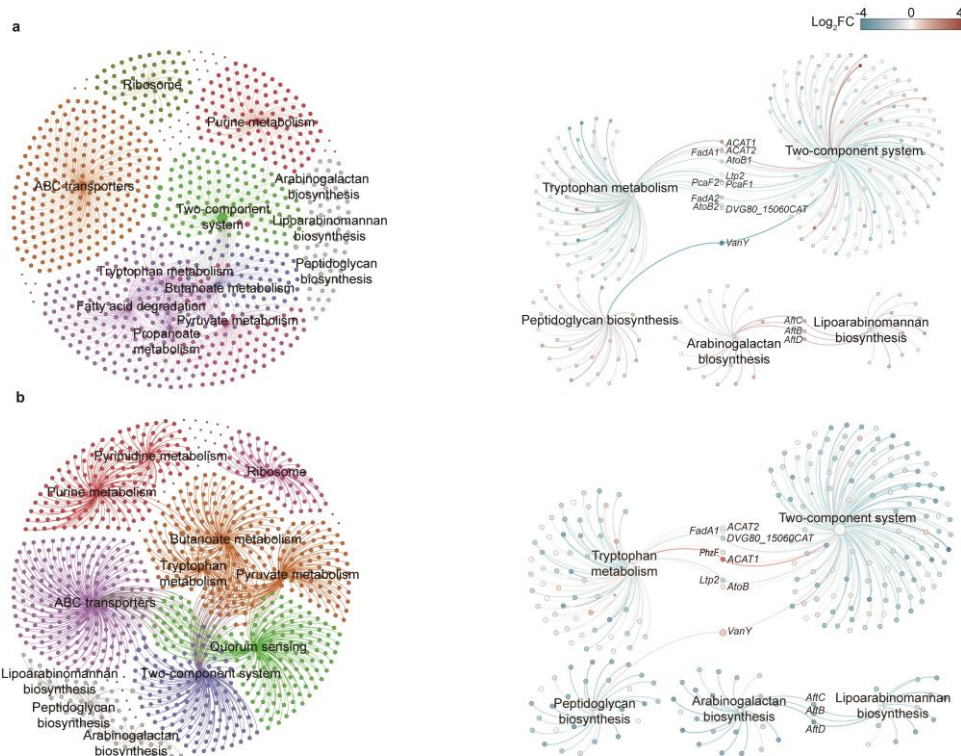
Supplementary Fig. 7. Concentrations of HHQ in soils of pot experiment. Bar plots represent the average value, and error bars represent the standard deviation (n = 3 biological replicates). Different letters indicate significant differences in variance analysis (one-way ANOVA, $P < 0.05$) after multiple comparisons (Two-sided Fisher's LSD test). CK: no-inoculation, Rh: inoculation with *R. erythropolis*, Ps: inoculation with *P. aeruginosa*, RP: inoculation with co-cultured *R. erythropolis* and *P. aeruginosa*. Source data are provided as a Source Data file.



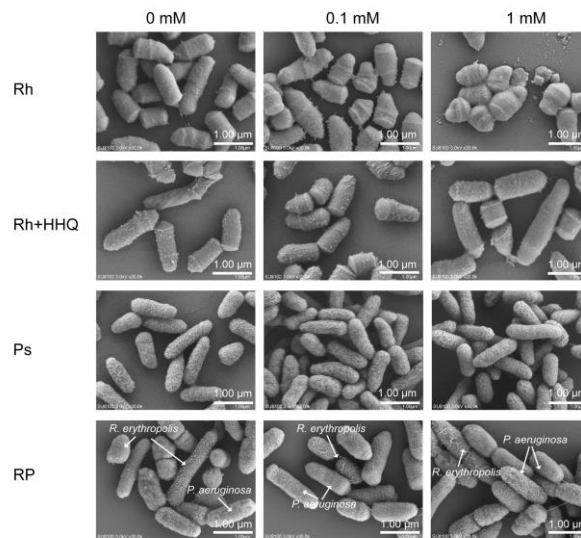
Supplementary Fig. 8. Concentrations of HHQ in sterilized systems. Temporal changes of HHQ concentrations in sterilized acidic soil (**a**) and sterilized clay-based system (**b**). The scatter dot plot represent the average value, and error bars represent the standard deviation (n = 3 biological replicates). The two-sided unpaired *t* test was used for statistical significance testing. **P* < 0.05, ***P* < 0.01, and ****P* < 0.001. HHQ: initiated with the addition of 20 μg L⁻¹ HHQ, HHQ+Rh: inoculation with *R. erythropolis* and 20 μg L⁻¹ HHQ, CK: no-inoculation, Rh: inoculation with *R. erythropolis*, Ps: inoculation with *P. aeruginosa*, RP: inoculation with co-cultured *R. erythropolis* and *P. aeruginosa*. Source data are provided as a Source Data file.



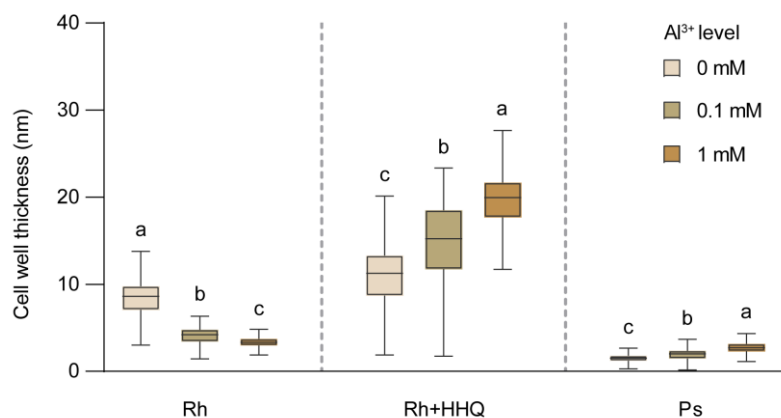
Supplementary Fig. 9. Top 10 enriched pathways for differentially expressed genes (DEGs) in *P. aeruginosa* and *R. erythropolis* under different treatments. (a-b), DEGs in mono-culture of *P. aeruginosa* with or without the addition of 0.1 mM Al³⁺ (a), and in co-culture versus mono-culture of *P. aeruginosa* with the addition of 0.1 mM Al³⁺ (b). (c-d), DEGs in mono-culture of *R. erythropolis* with or without the addition of 0.1 mM Al³⁺ (c), and co-culture versus mono-culture of *R. erythropolis* with the addition of 0.1 mM Al³⁺ (d). Top 10 enriched metabolic pathways for DEGs (Fold Change > 1.5 and FDR value < 0.05) were counted. The numbers on the bars reflect the count of DEGs in each pathway.



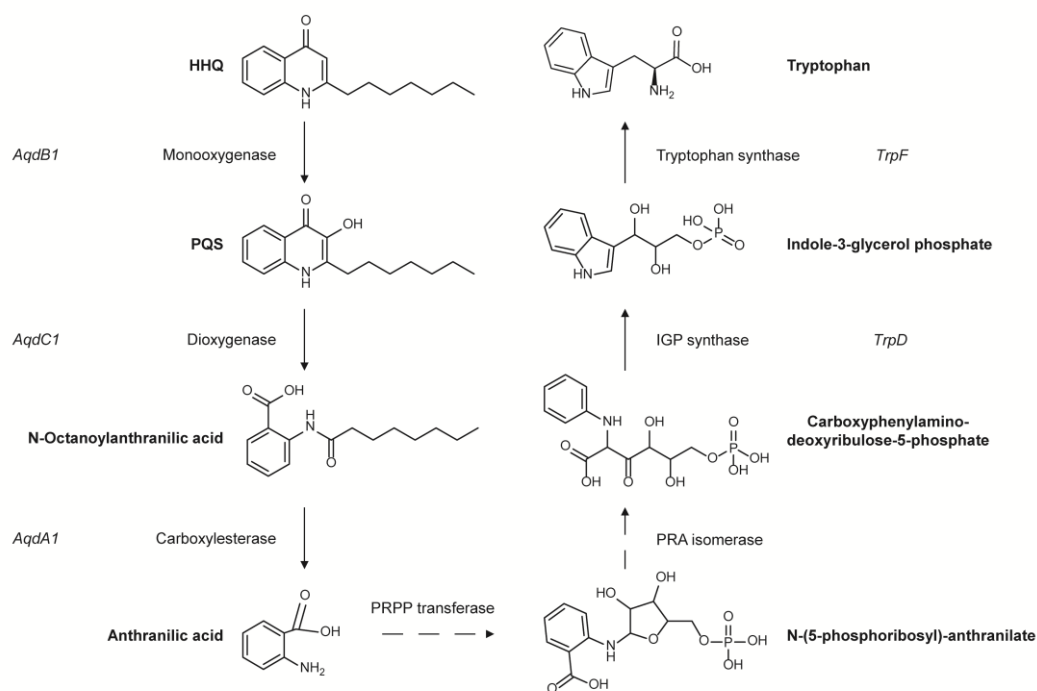
Supplementary Fig. 10. Network analysis of top 10 enriched pathways for differentially expressed genes (DEGs) in *R. erythropolis*. **a**, Modular analysis of top 10 pathway DEGs in co-culture and mono-culture with the addition of 0.1 mM Al^{3+} . **b**, Modular analysis and subnetwork analysis of top 10 pathway DEGs in mono-culture of *R. erythropolis* with or without the addition of 0.1 mM Al^{3+} . The subnetworks (right) in **a** and **b** show the connections between tryptophan metabolism pathway (ko00380), two-component system pathway (ko02020), and cell wall components pathway which includes peptidoglycan (ko00550), arabinogalactan (ko00572), and lipopolysaccharide (ko00571) biosynthesis pathway.



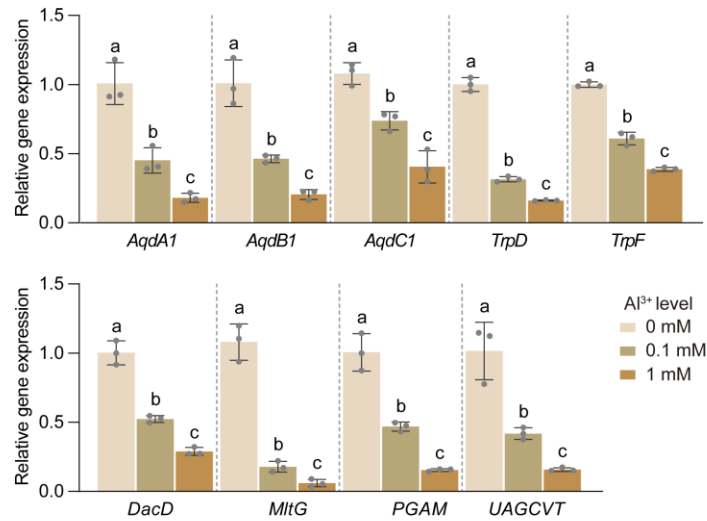
Supplementary Fig. 11. Scanning electron microscopy (SEM) images of cell morphological analysis. The images representative of 3 experiments. Rh: mono-culture of *R. erythropolis*, Rh+HHQ: mono-culture of *R. erythropolis* with the addition of 20 μ M HHQ, Ps: mono-culture of *P. aeruginosa*. RP: inoculation with co-cultured *R. erythropolis* and *P. aeruginosa*. The scale bar is 1.00 μ m.



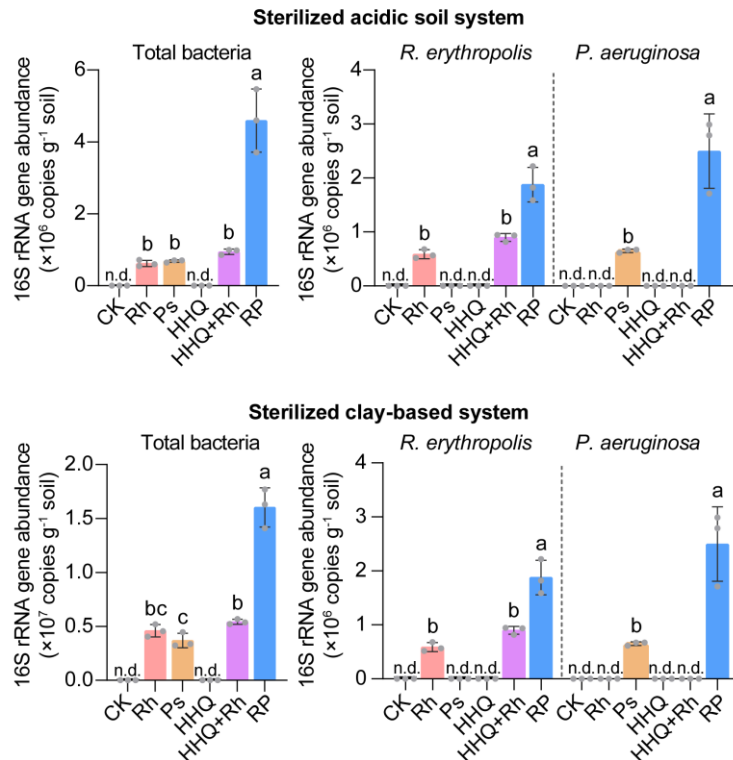
Supplementary Fig. 12. Cell wall thickness among different treatments. The scanning range encompasses an area of 100 nm × 100 nm, involving a total of 16,384 points. The horizontal bars within the box plots represent medians, the tops and bottoms of the boxes represent the 75th and 25th percentiles, respectively, and the upper and lower whiskers extend to the maximum and minimum values, respectively. Different letters indicate significant differences ($P < 0.05$, One-way ANOVA, two-sided Fisher's LSD test). Rh: inoculation with *R. erythropolis*, HHQ+Rh: inoculation with *R. erythropolis* and 20 $\mu\text{g L}^{-1}$ HHQ, Ps: inoculation with *P. aeruginosa*. Source data are provided as a Source Data file.



Supplementary Fig. 13. Key steps in oxidation process of HHQ and biosynthesis of tryptophan from anthranilate metabolism in *R. erythropolis*. Solid lines represent the transcription levels of genes encoding enzymes that were measured in this study, while dashed lines represent those that were not measured.

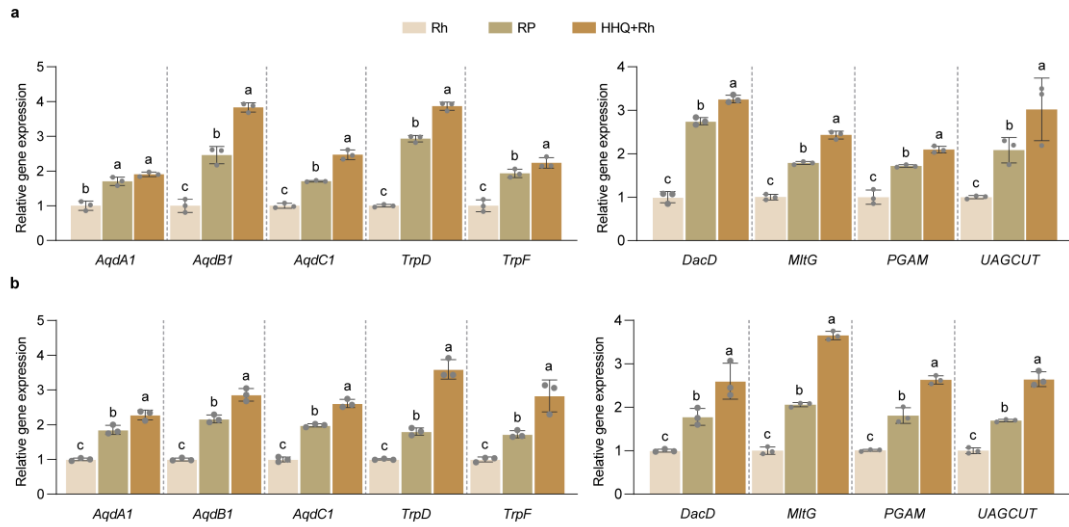


Supplementary Fig. 14. Relative expression levels of selected key genes in *R. erythropolis* under different added Al^{3+} concentrations without HHQ addition. Bar plots represent the average value, and error bars represent the standard deviation, $n = 3$ biological replicates. Different letters indicate significant differences in variance analysis (one-way ANOVA, $P < 0.05$) after multiple comparisons (Two-sided Fisher's LSD test). Source data are provided as a Source Data file.

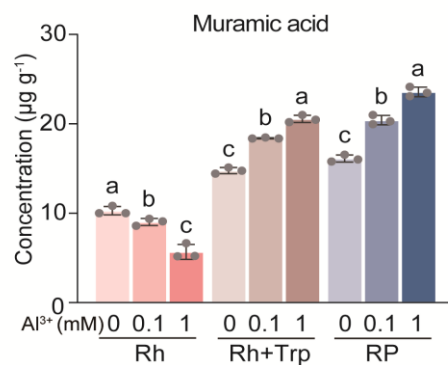


Supplementary Fig. 15. The bacterial abundance in different sterilized systems.

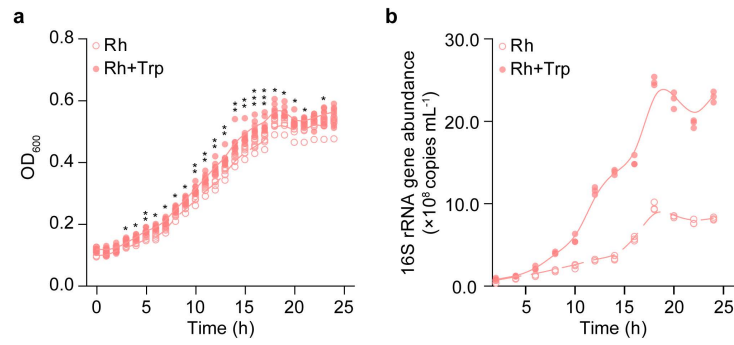
The absolute abundance of total bacteria, *R. erythropolis*, and *P. aeruginosa* in the rice (Nanjing 46) rhizosphere soil at 7 days in sterilized clay-based system and sterilized acid soils (n = 3 biological replicates). Bar plots represent the average value, and error bars represent the standard deviation. Different letters indicate significant differences in variance analysis (one-way ANOVA, $P < 0.05$) after multiple comparisons (Two-sided Fisher's LSD test). CK: no-inoculation, Rh: inoculation with *R. erythropolis*, Ps: inoculation with *P. aeruginosa*, HHQ: addition of 20 $\mu\text{g L}^{-1}$ HHQ, HHQ+Rh: inoculation with *R. erythropolis* and 20 $\mu\text{g L}^{-1}$ HHQ, RP: inoculation with co-cultured *R. erythropolis* and *P. aeruginosa*. Source data are provided as a Source Data file.



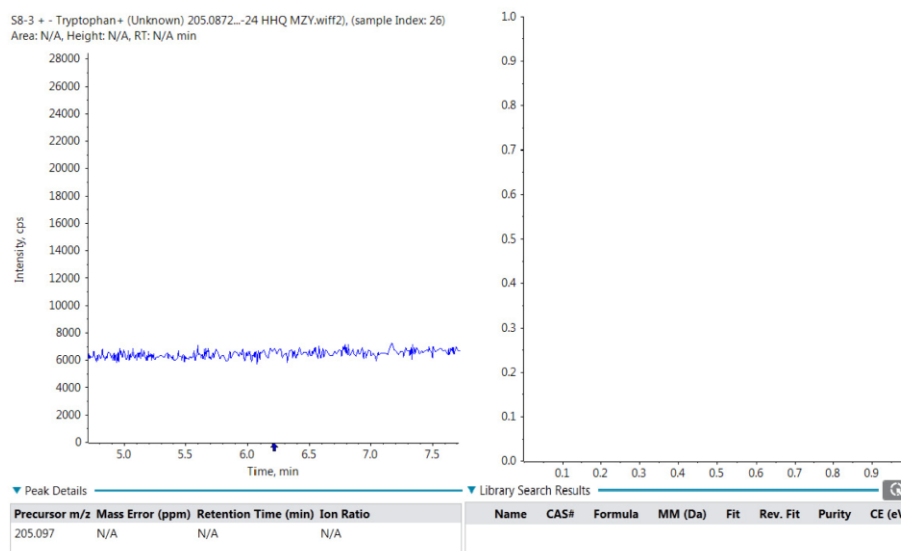
Supplementary Fig. 16. Transcriptional expression analysis of HHQ-mediated *R. erythropolis* functional genes in sterilized substrate system. Relative expression levels in sterilized clay-based system **a** and sterilized acidic soil at 7 days **b**. Bar plots represent the average value, and error bars represent the standard deviation, $n = 3$ biological replicates. Different letters indicate significant differences in variance analysis (one-way ANOVA, $P < 0.05$) after multiple comparisons (Two-sided Fisher's LSD test). Rh: inoculation with *R. erythropolis*, RP: inoculation with co-cultured *R. erythropolis* and *P. aeruginosa*, HHQ+Rh: inoculation with *R. erythropolis* and $20 \mu\text{g L}^{-1}$ HHQ. Source data are provided as a Source Data file.



Supplementary Fig. 17. Muramic acid concentrations under treatments with different Al³⁺ addition concentrations. Bar plots represent the average value, and error bars represent the standard deviation (n = 3 biological replicates). Different letters indicate significant differences in variance analysis (one-way ANOVA, $P < 0.05$) after multiple comparisons (Two-sided Fisher's LSD test). Rh: mono-culture of *R. erythropolis*, Rh+Trp: mono-culture of *R. erythropolis* with the addition of 20 µM HHQ, RP: co-culture of *R. erythropolis* and *P. aeruginosa*. Source data are provided as a Source Data file.

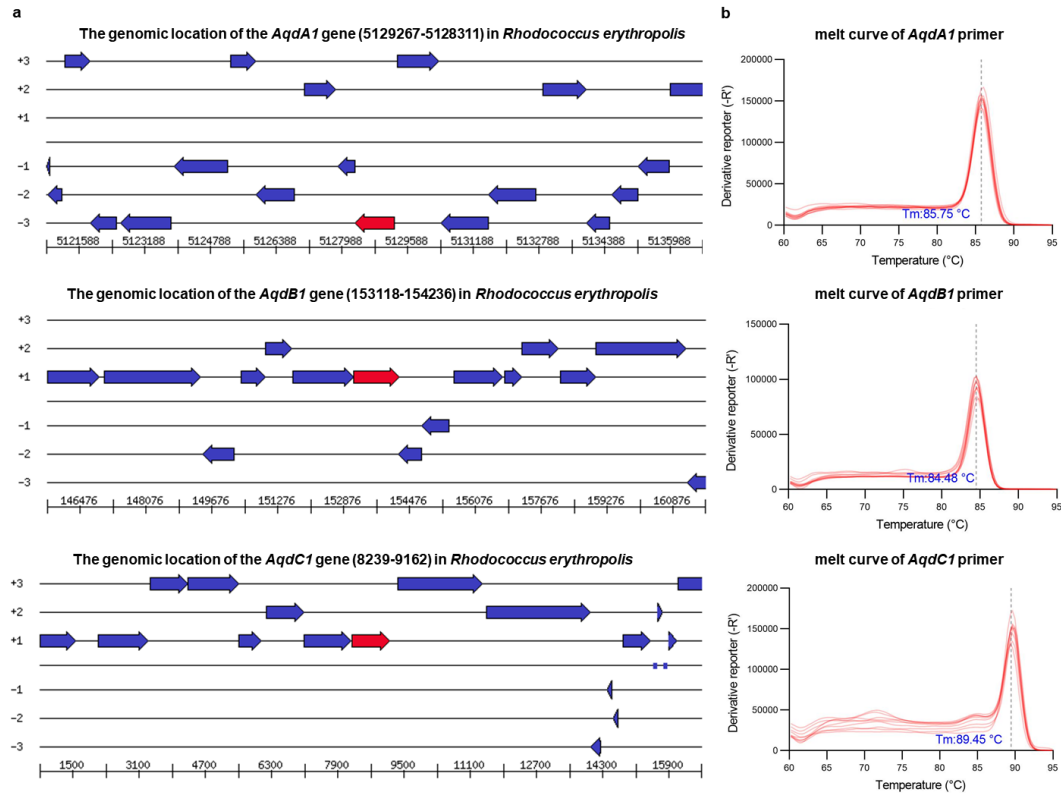


Supplementary Fig. 18. Promoting effect of tryptophan addition on *R. erythropolis* growth. **a**, Growth density curves of *R. erythropolis* with the addition of 0.5 mM tryptophan (Rh+Trp) and without tryptophan addition (Rh) (n = 10 biological replicates). **b**, Absolute abundance of *R. erythropolis* with and without tryptophan addition (n = 3 biological replicates). The two-sided unpaired *t* test was used for statistical significance testing in **a**. **P* < 0.05, ***P* < 0.01, and ****P* < 0.001. Source data are provided as a Source Data file.

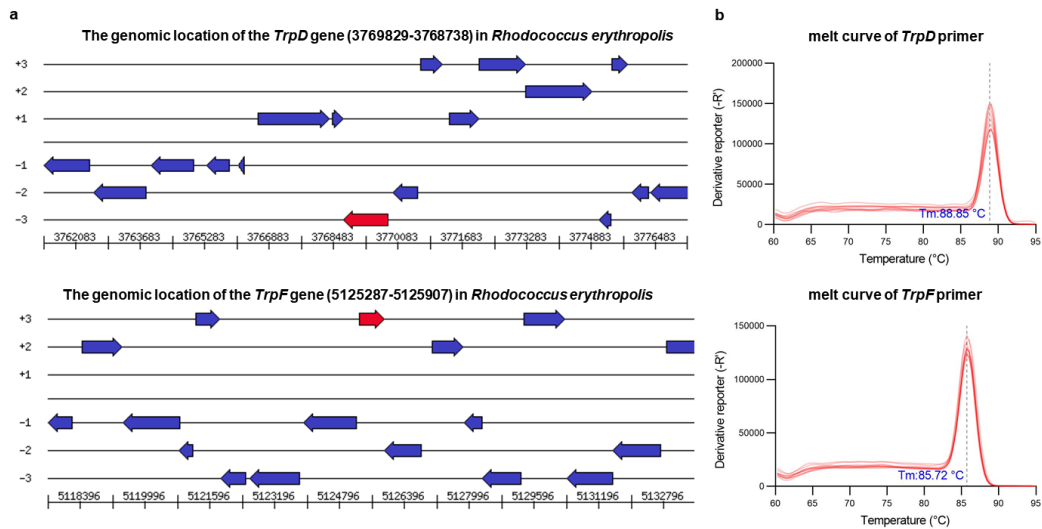


Supplementary Fig. 19. The primary and secondary spectra of tryptophan peak.

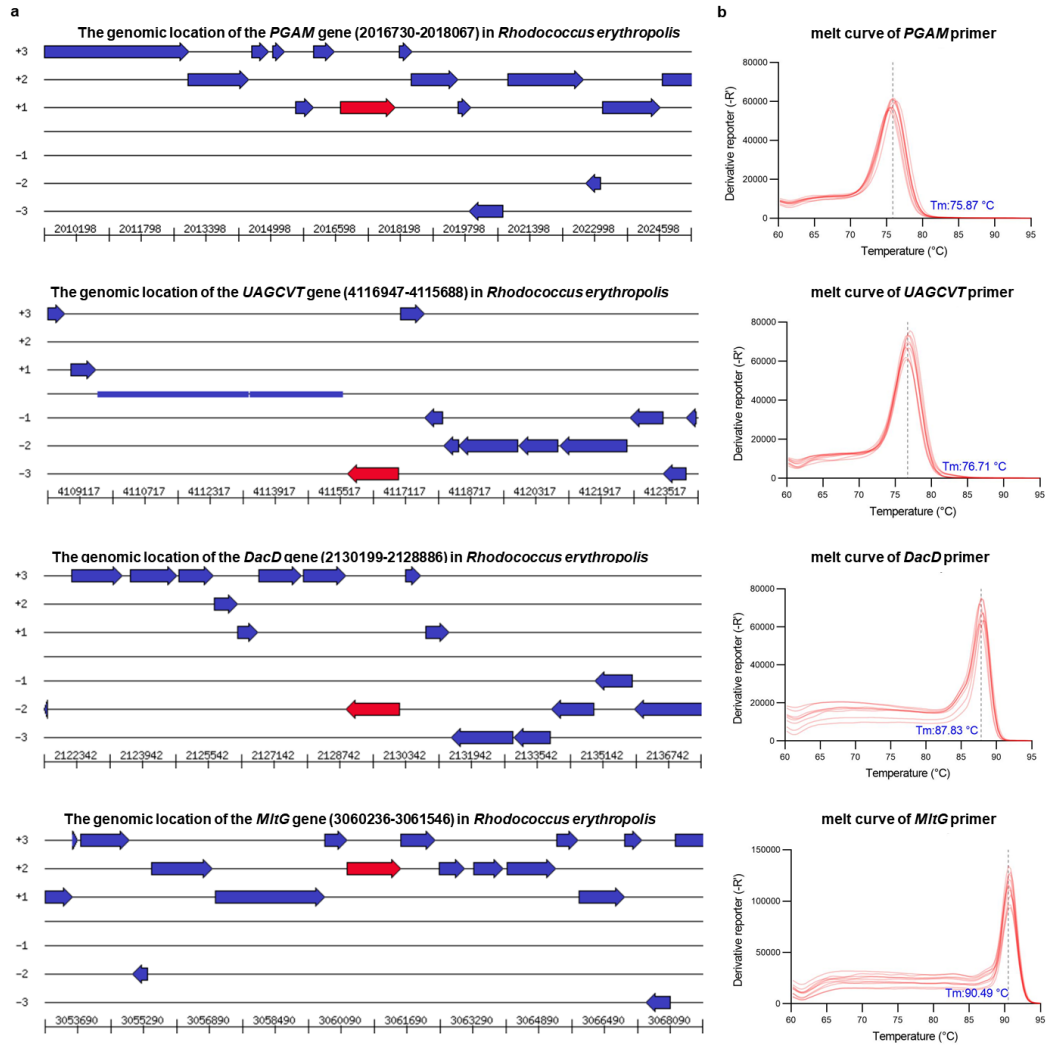
The tryptophan signal was not identified by the primary and secondary spectrogram signal.



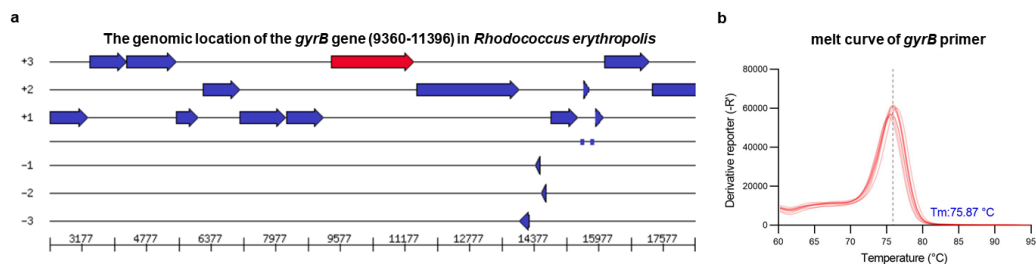
Supplementary Fig. 20. Genomic sequence mapping of alkylquinolone-specific catabolic enzymes (*AqdA1*, *B1*, *C1*) and specific primer melt curves for gene regulation. **a**, the genomic location of *AqdA1*, *AqdB1* and *AqdC1* in *Rhodococcus erythropolis*. **b**, the melt curve of each surveyed primer, n = 10 biological replicates. Detailed nucleotide sequence information is provided in Supplementary Data 5. For additional primer design and evaluation results using Primer premier 6.0, please refer to Supplementary Data 3 and 4. Source data are provided as a Source Data file.



Supplementary Fig. 21. Genomic sequence mapping of tryptophan operons (*TrpD* and *TrpF*) and specific primer melt curves for gene regulation. a, the genomic location of *TrpD* and *TrpF* in *Rhodococcus erythropolis*. **b**, the melt curve of each surveyed primer, n = 10 biological replicates. Detailed nucleotide sequence information is provided in Supplementary Data 5. For additional primer design and evaluation results using Primer premier 6.0, please refer to Supplementary Data 3 and 4. Source data are provided as a Source Data file.



Supplementary Fig. 22. Genomic sequence mapping of cell wall synthesis pathways (*PGAM*, *UAGCVT*, *DacD* and *MltG*) and specific primer melt curves for gene regulation. a, the genomic location of *PGAM*, *UAGCVT*, *DacD* and *MltG* in *Rhodococcus erythropolis*. **b**, the melt curve of each surveyed primer, n = 10 biological replicates. Detailed nucleotide sequence information is provided in Supplementary Data 5. For additional primer design and evaluation results using Primer premier 6.0, please refer to Supplementary Data 3 and 4. Source data are provided as a Source Data file.



Supplementary Fig. 23. Genomic sequence mapping of house-keeper gene (*gyrB*) and specific primer melt curve for gene regulation. a, the genomic location of *gyrB* in *Rhodococcus erythropolis*. **b**, the melt curve of primer, n = 6 biological replicates. Detailed nucleotide sequence information is provided in Supplementary Data 5. For additional primer design and evaluation results using Primer premier 6.0, please refer to Supplementary Data 3 and 4. Source data are provided as a Source Data file.

Supplementary Note 1. Phosphorus (P)-solubilizing ability of co-culture and mono-cultures under aluminium (Al) stress

Different culture conditions were employed using modified minimal media (MM) supplemented with 1 g L^{-1} sodium phytate (organic fixed P, MM-Po) and 1 g L^{-1} tricalcium phosphate (inorganic fixed P, MM- Ca_3P). The sensitivity of *R. erythropolis* to Al increased as the concentration of added Al^{3+} rose from 0, 0.1 to 1 mM, regardless of P supplementation conditions. The available phosphorus (AP) content showed a significant decrease, with conversion rates of 8.83%, 7.83%, and 5.62%, respectively (Supplementary Fig. 6a). In contrast, *P. aeruginosa* maintained its Al tolerance and P-solubilizing ability especially in MM-Po, with stable conversion rates of 11.25 to 11.60%. Following co-culture, the AP content further increased with increased Al^{3+} concentrations, with conversion rates of 11.45% to 12.92% in MM-Po and 0.80% to 2.34% in MM- Ca_3P , respectively, indicating enhanced Al tolerance and P-solubilizing ability of SynCom.

Likewise, pot experiment confirmed that SynCom treatment resulted in the highest AP content and the lowest total phosphorus (TP) compared to single inoculation and the control (CK) (Supplementary Fig. 6b). The AP concentrations were ranked as RP ($99.47 \pm 1.10\text{ mg kg}^{-1}$) > Ps ($89.40 \pm 0.53\text{ mg kg}^{-1}$) > Rh ($78.53 \pm 3.58\text{ mg kg}^{-1}$) > CK ($73.00 \pm 7.64\text{ mg kg}^{-1}$). Due to a subsequent absorption by plant roots, there was an inverse trend observed in the TP concentration in the pots, with CK ($548.70 \pm 3.30\text{ mg kg}^{-1}$) > Rh ($491.90 \pm 9.93\text{ mg kg}^{-1}$) > Ps ($489.30 \pm 1.99\text{ mg kg}^{-1}$) > RP ($471.4 \pm 3.80\text{ mg kg}^{-1}$).

These results underscored that under acidic Al stress, the SynCom effectively enhanced the phosphorus-solubilizing ability of the individual strains.

Supplementary Note 2. Production and degradation of HHQ by

SynCom in acidic soil and clay-based system

Measurement of HHQ concentration

The pot experiments in acidic soils under natural conditions comprised four treatments: non-inoculation (CK), single strain inoculation (*R. erythropolis* and *P. aeruginosa*), and SynCom inoculation. The results indicated that, compared to the non-inoculated soil ($18.23 \pm 0.58 \text{ mg kg}^{-1}$), the inoculation with *R. erythropolis* significantly reduced the HHQ concentration by 57.7%, bringing it down to $7.71 \pm 1.18 \text{ mg kg}^{-1}$. In contrast, inoculation with *P. aeruginosa* led to an approximate 3.8-fold increase in HHQ concentration, reaching $70.41 \pm 8.72 \text{ mg kg}^{-1}$ (Supplementary Figure 7). Following SynCom inoculation, the HHQ concentration ($44.19 \pm 5.07 \text{ mg kg}^{-1}$) was lower than that observed with *P. aeruginosa* inoculation but remained higher than in natural soil and in soil with *R. erythropolis* inoculation.

Additionally, we measured the temporal dynamics of HHQ production and degradation in both and sterilized acidic soil and clay-based substrate. Here, an initial HHQ concentration was established to mimic natural soil levels, and *R. erythropolis* was introduced to evaluate its role in the degradation process. Parallel treatments included inoculation with *P. aeruginosa* and SynCom. *R. erythropolis* substantially reduced the HHQ concentration in both systems over 7 days by 74.75% and 76.91%, respectively (Supplementary Fig. 8). Meanwhile, the elevated HHQ levels resulting from *P. aeruginosa* inoculation was partially degraded by *R. erythropolis* when inoculated with SynCom, leading to reductions of approximately 52.91% and 53.91%, respectively.

Key genes expressions involved in HHQ metabolic pathways

To indicate the exceptional metabolic capability of *R. erythropolis* to degrade HHQ, we further investigated the bacterial colonization and key genes involved in HHQ metabolic pathways under sterilized acid soil and clay-based systems. Similar to observations under natural soil conditions (Fig. 1a, b), we observed a significant

increase in the abundance of *R. erythropolis* and *P. aeruginosa* with SynCom inoculation compared to their individual inoculation (Supplementary Fig. 15). Additionally, the presence of HHQ and co-culturing with *P. aeruginosa* led to increased expression levels of key genes in *R. erythropolis* that are potentially involved in the degradation of the quinolone compound (*AqdA1*, *B1*, and *C1*), the tryptophan operons (*TrpD* and *TrpF*), and the cell wall-related substance synthesis (*DacD*, *MltG*, *PGAM*, and *UAGCVT*) (Supplementary Fig. 16).

Taken together, these results further underscore the efficient ability of *R. erythropolis* to degrade HHQ, both in liquid medium and soil matrix.

Supplementary Method 1. Sequential chemical extraction of soil P

Hedley P fractionation procedure and its modifications (Tiessen) are designed to estimate soil P pools^{1,2,3}. Briefly, P was fractionated into seven fractions, including resin-P (extracted with deionized water and anion exchange resin), NaHCO₃-Pi and NaHCO₃-Po (extracted with 0.5 M NaHCO₃), NaOH-Pi and NaOH-Po (extracted with 0.1 M NaOH), HCl-Pi (extracted with 0.5 M HCl) and residual-P (digested with H₂SO₄ and H₂O₂). NaHCO₃-Po was calculated from the difference between NaHCO₃-total P (from digestion) and NaHCO₃-Pi. NaOH-Po was calculated from the difference between NaOH-total P (from digestion) and NaOH-Pi. Residual P indicated the occluded P pool. Available P was calculated as the sum of resin-P and NaHCO₃-Pi. Total P was calculated as the sum of seven P fractions. The inorganic P concentration in each extract was determined by measuring absorbance at 700 nm using a UVmini-1240 ultraviolet spectrophotometer (Shimadzu Co., LTD., China) using the ascorbic acid molybdenum blue method.

Supplementary Method 2. Determination of P-solubilizing ability of bacteria

In this study, we utilized modified minimal media (MM) supplemented with organic and inorganic fixed P forms⁴. The MM with organic fixed P (MM-Po) was prepared by adding 10 g of glucose, 1 g sodium phytate, 0.5 g of (NH₄)₂SO₄, 0.3 g of KCl, 0.3 g of NaCl, 0.03 g MnSO₄·H₂O, 0.03 g of FeSO₄·7H₂O, and 0.03 g of MgSO₄·7H₂O into 1000 mL of ultrapure water. The MM with tricalcium phosphate (MM-Ca₃P), representing inorganic fixed P, was prepared by adding 1 g of Ca₃(PO₄)₂ as the sole P source.

R. erythropolis and *P. aeruginosa* cultures, previously grown overnight in LB media, were washed for three times with ultrapure water to eliminate residual phosphate. Then 200 µL of the prepared bacterial suspension was inoculated in 20 mL of MM-Po and MM-Ca₃P, each performed in triplicate. The Al concentration gradients were set to 0, 0.1, and 1mM. Following a 5-day incubation period at room temperature, the bacterial suspensions were centrifuged at 5,000 rpm. The supernatants were filtered through a 0.22 µm filter to remove any bacteria and Ca₃P. The concentrations of the released water-soluble phosphate, considered as available P, were determined using the ascorbic acid molybdenum blue method by measuring absorbance at 700 nm with a UVmini-1240 ultraviolet spectrophotometer (Shimadzu Co., LTD., China).

Supplementary Method 3. Al concentration in rice roots

A total of 0.20 g of rice root dried sample were weighed and transferred to a digestion tube. 6 mL of concentrated nitric acid (70 %, J.T.Baker, Inc., America) and 2 mL of hydrogen peroxide (30 %, J.T.Baker, Inc., America) were added to the digestion tube, 105 °C for 7 h. After cooling for 20 min, the digestion tube was taken out and move to a precise temperature-controlled electric digestion device (East Aviation Science Instrument Co., Ltd., Beijing, China) at 300 °C for acid removal. Ultra-pure water was used to wash samples and then diluted to a constant volume of 10 mL. Blank samples and standard rice samples (GBW10010) (Institute of Geophysical and Geochemical Exploration, Beijing, China) were digested with the same method. Each sample was

determined via inductively coupled plasma–optical emission spectrometry (ICP–OES, PerkinElmer Avio 200, Waltham, USA).

Supplementary Method 4. HHQ quantification in pure cultures

A total of 1 μL of supernatant from each group was analysed using an Agilent 1260 high-performance liquid chromatograph (Agilent Technologies, Palo Alto, CA, USA) coupled with a Triple TOF 5600 mass spectrometer (AB SCIEX, Foster City, CA, USA). Separation was performed using an ACQUITY BEH C18 column (2.1 mm \times 100 mm, 1.7 μm ; Waters, Milford, MA, USA). The mobile phase consisted of 2 mM ammonium acetate solution (A) and acetonitrile (B), and the elution program was as follows: initial flow rate of 0.4 mL min^{-1} , 20% phase B was maintained for 1.5 min, then increased from 20% phase B to 70% B phase within 10.5 min, followed by a linear increase to 100% phase B within 1 min, maintained for 9 min, and then decreased to 20% within 1 min and equilibrated for 3 min. The mass spectrometer used information-dependent acquisition mode (IDA). The gas and other mass spectrometer settings were as follows: gas 1, nitrogen (55 psi); gas 2, nitrogen (55 psi); ion spray voltage, 5500 V (positive) and -4500 V (negative); ion source temperature, 550 $^{\circ}\text{C}$; and curtain gas, nitrogen (25 psi). Each cycle included a TOFMS spectrum acquisition of 200 ms (mass range of 50–1250 aum). Data analysis was performed using Analyst[®] and MultiQuant[™] Software (version 1.6) from SCIEX.

Supplementary Method 5. HHQ quantification in soil matrixes and clay-based substrate

A total of 10 g dried sample were mixed with diatomite. Stainless steel extraction cells (22 mL) were packed with an in-cell absorbent (quartz sand and florisil) and soil samples. All extracted procedures were by used of accelerated solvent extraction (HPFE 06S, RayKol, Raykol group Corp. Ltd., China). Cells were extracted with a 1:1 solution of ethyl acetate acidified by acetic acid ($v/v=1:1000$) and n-Hexane at a temperature of

100 °C and 1600 psi (11Mpa) with a preheat time of 5 min, a flush volume of 50% and 2 cycles with a static time of 30 min each. The resulting extracts were reduced under rotary evaporation and gentle stream of nitrogen, and then dissolved into 1 mL with Methanol. After passing through a 0.22 µm membrane, the concentration of HHQ was detected using an AB 5500 liquid chromatography coupled with tandem triple-quadrupole mass spectrometry (LC–MS/MS) (AB SCIEX LLC, MA, USA). Six laboratory blanks and matrix spikes were extracted for quality assurance purposes.

Agilent Proshell 120 C-18 column (150 mm × 3.0 mm, 2.7 µm, Agilent Technologies Inc., USA) was used for separation. The mobile phase consisted of a water solution containing 0.1% formic acid (A) and acetonitrile (B), with a flow rate of 0.3 mL min⁻¹ and an injection volume of 1 µL. The elution program was as follows: initially 35% phase B was maintained for 1.0 min, then increased to 98% within 5 min, followed by a maintenance period of 1.0 min. Subsequently, it decreased from 98% phase B to 35% within 0.5 min and balanced for 3.5 min. The limit of detection limit (LOD) of the instrument was determined by external standards (HHQ) for quantitative analysis. The mass spectrometry information of the external standard muramic acid was as follows: Q1=244.0, Q3=159.0, DP=-20 V, and CE=-32 eV (quantification); Q1=244.0, Q3=172.0, DP=-20 V, and CE=-18 eV (qualitative). The method LOD refers to a signal peak that is three times greater than the background noise of the instrument. In this study, the LOD of HHQ was 0.02 µg L⁻¹, and the recovery rate was 95.34%-101.67%.

Supplementary references

1. Hedley, M. J., Stewart, J. W. B. & Chauhan, B. S. Changes in inorganic and organic soil-phosphorus fractions induced by cultivation practices and by laboratory incubations. *Soil Sci Soc Am J* **46**, 970-976, (1982).
2. Tiessen, H. Characterization of available P by sequential extraction. *Soil sampling and methods of analysis*, (1993).
3. Wang, Y. *et al.* Reduced phosphorus availability in paddy soils under atmospheric CO₂ enrichment. *Nat Geosci* **16**, 162-168, (2023).
4. Li, H. Z. *et al.* D₂O-isotope-labeling approach to probing phosphate-solubilizing bacteria in complex soil communities by single-cell raman spectroscopy. *Anal Chem* **91**, 2239-2246, (2019).